Cost-effective time-lapse seismic characterization of fracture dynamic changes

Hao Hu[1], Ying Zhang[2], Xinding Fang[3,4], Tianrun Chen[3], Yingcai Zheng[4]*

1. *School of Geoscience, University of Oklahoma, Norman, OK*
2. *U.S. Geological Survey, Menlo Park, CA*
3. *SensorEra Inc., Sugar Land, TX*
4. *Department of Earth and Atmospheric Sciences, University of Houston, Houston, TX*

Summary

Understanding subsurface fracture dynamic changes is crucial for optimizing fossil and geothermal energy production and assessing the safety of carbon sequestration. However, a conventional time-lapse-3D (4D) seismic survey is expensive for capturing dynamic fracture changes at short time intervals (~hours) within a typical production cycle (~ days). To address this challenge, we propose a cost-effective yet reliable solution using a novel repeated source time-lapse seismic acquisition combined with the elastic double-beam (EDB) method. This approach utilizes spatially sparse 3-component seismic nodes and a single permanent source. The EDB method, applied to this seismic acquisition geometry, can effectively detect spatial variations in subsurface fracture properties. We evaluate this solution using elastic synthetic datasets from layered models containing two different fracture sets: one horizontally extended and the other depth extended. The results demonstrate that the EDB method, when applied to this cost-effective 4D seismic setup, can accurately resolve both fracture sets and their spatial variations. This innovative and affordable solution holds significant potential for applications in energy production optimization and carbon sequestration monitoring.

Introduction

Dynamic changes of subsurface fractures caused by energy production and CO2 injection are a key indicator to evaluate the production efficiency and guide the drilling strategies (Hubbert and Willis 1957, Barton et al. 1995, Nelson 2001, Montgomery and Smith 2010, Shukla et al. 2010, Orangi et al. 2011, Caulk et al. 2016). Subsurface fractures can introduce seismic anisotropy in reflected/transmitted elastic waves and fracture-related scattered waves. This relationship between subsurface fractures and seismic waves can be used to characterize the fractures. Commonly used seismic methods for fracture characterization utilize seismic anisotropy, including the AVO/AVAZ analysis (amplitude variation with offset and azimuth) for the reflected waves (e.g., Rüger and Tsvankin 1997, Lynn et al. 1999, Perez et al. 1999, Thomsen 1999, Stewart et al. 2002, 2003, Vasconcelos and Grechka 2007, Far et al. 2014) and shear-wave splitting (e.g., Crampin 1985, Tatham et al. 1992, Vetri et al. 2003, Long 2013, Verdon and Wustefeld 2013). However, such anisotropy-related methods assume the fractures are spatially uniformly alligned, which may not hold true for natural fractures (e.g., David et al. 1990). Non-uniformly distributed fractures could generate strong multiply-scattered seismic waves that may introduce errors in the AVAz analysis (Fang et al. 2017).

Another category of fracture characterization methods is imaging-based, which uses scattered waves from the fractures to image the fracture networks, including stacking-based methods (e.g., Willis et al. 2006, Fang et al. 2014a) and migration methods (e.g., Landa et al. 2008, Landa et al. 2011, Klokov and Fomel 2012, Landa 2012, Landa et al. 2013, Schoepp et al. 2015, Protasov et al. 2016, Silvestrov et al. 2016, Hu et al. 2023). However, imaging-based methods often suffer from high computational costs or limited spatial resolution, restricting their practical applicability in complex subsurface structures.

Besides the seismic anisotropy-related methods and imaging-based methods, the double-beam (DB) method has been developed to characterize fractures by using the interference pattern of multiply-scattered waves among fractures (e.g., Zheng, Fang, and Fehler 2013, Zheng, Fang, Fehler, et al. 2013, Hu and Zheng 2017, 2018, Hu et al. 2018, Hu et al. 2021). This method has been validated through various synthetic models containing multiple sets of fractures with random spacings and complex compliance patterns (Hu and Zheng 2017, 2018, Hu et al. 2018). In addition, Hu et al. (2021) extended the DB method to use elastic waves (also called elastic DB) that can further self-cross-validate the results for enhancing accuracy and reliability.

In the meantime, time-lapse seismic acquisition, processing, and imaging have been developed to understand and monitor the subsurface changes due to the production activities (e.g., Johnston 1997, Harvey et al. 2022). However, due to the expensive cost of 3D seismic acquisition, the conventional time-lapse (4D) seismic monitoring only took a few times of data acquisition at the same region over specific intervals during production. To reduce the cost of 4D seismic survey, Shang and Huang (2012) optimized the seismic survey for the time-lapse monitoring using elastic wave sensitivity analysis. Oghenekohwo et al. (2017) employed the distributed compressive sensing to reduce the density of geophones. Such 4D seismic surveys can only provide the subsurface changes at a limited number of time points. Permanent source seismic acquisition has emerged as a method for real-time and continuous monitoring of the subsurface reservoir dynamic changes through using

10.1190/image2025-4301170.1

repeated sources and long-term deployed seismic nodes (Meunier et al. 2000, Arts et al. 2013, Berron et al. 2015, Spackman and Lawton 2018, Spackman et al. 2019). For example, White et al. (2015) monitor changes in surface waves from a permanent source; Nakatsukasa et al. (2016) measure the time shifts and amplitude differences in the recorded data from a permanent source. While 4D seismic with permanent sources and sparsely distributed seismic nodes could be a feasible and cost-effective solution for monitoring projects in a short period (~months), this approach may have limited angular coverage for deep subsurface reservoirs.

In this study, we propose integrating the elastic DB (EDB) method with cost-effective 4D seismic acquisition using a single permanent source to monitor subsurface fracture dynamic changes. During production, the primary focus is on regions surrounding the well at the production depth. This localized targeting makes 4D seismic acquisition with a single permanent source a viable approach for capturing fracture dynamic changes using the EDB method. To optimize illumination of production-relevant targets, the permanent source can be strategically positioned near the wellhead, while seismic nodes should be distributed with a sufficient offset range to enhance the monitoring aperture.

In this abstract, we provide a concise overview of the elastic double-beam (EDB) method. We then evaluate the feasibility and accuracy of our proposed cost-effective solution using two synthetic models with fracture sets of varying depths and lateral extents. Subsequently, we apply the EDB method to these models, analyze the results, and discuss the applicability and accuracy of the proposed approach.

Method: Elastic double-beam

Zheng, Fang, Fehler, et al. (2013) proposed the DB method using seismic acoustic waves (P-P waves) to invert for the distribution of subsurface fractures via two focused beams, source side and receiver side, from the acquisition surface to subsurface targets. Hu and Zheng (2018) and Hu et al. (2018) developed the DB method for non-flatten fractured reservoirs and tested its feasibility for fractures with random spacings. Hu et al. (2021) further developed the DB method for elastic waves from 3-component recordings. The elastic DB (EDB) method theoretically utilizes the relationship between the incident P waves and the scattered P waves and S waves:

$$\mathbf{k}_{PT}^{rcv} = \mathbf{k}_{PT}^{src} + n\frac{2\pi}{a}\hat{\varphi}, \qquad n = 0, \pm1, \pm2, \dots, \qquad (1)$$

$$\mathbf{k}_{ST}^{rcv} = \mathbf{k}_{PT}^{src} + n\frac{2\pi}{a}\hat{\varphi}, \qquad n = 0, \pm1, \pm2, \dots, \qquad (2)$$

where $\mathbf{k}_{PT}^{rcv}$ and $\mathbf{k}_{PT}^{src}$ are the horizontal components of P-wave wavenumber from the receiver beam center ($\mathbf{k}_{P}^{rcv}$) and source beam center $\mathbf{k}_{P}^{src}$, respectively; $\mathbf{k}_{ST}^{rcv}$ is the horizontal component of scattered S-wave wavenumber from the receiver beam center ($\mathbf{k}_{ST}^{rcv}$); $\hat{\varphi}$ is the fracture orientation vector that is perpendicular to the fracture plane; a is the spacing between fracture plans.

These relations (Eq (1) and (2)) link the subsurface fracture geometry to the surface seismic data at varying source beam locations, receiver beam locations, and time. We then can set up the subsurface targets with interests and scan the fracture orientation, spacing, and the beam centers based on the velocity model to extract the possible scattered signals from the seismic records. For each target, the extracted signals could be stacked to form an interference pattern image (DB image) as a function of fracture spacings and orientations. Additionally, amplitudes in the DB image are proportional to the energy strength of the fracture-related scattered waves that are related to the fracture's local physical property (e.g., compliance) (e.g., Zheng, Fang, and Fehler 2013, Fang et al. 2014b, Hu et al. 2018). The implementation details can be found in Zheng, Fang, Fehler, et al. (2013) and Hu et al. (2021).

Examples

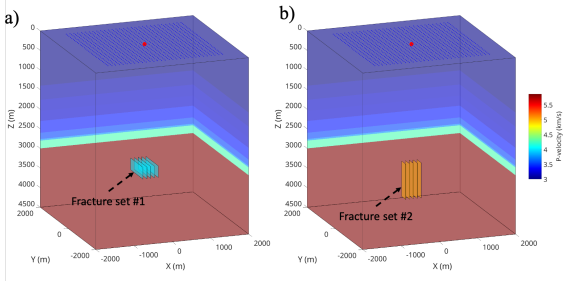

Figure 1. The velocity model contains the subsurface fractures and surface seismic acquisition. The red dot on the surface is the source, and the blue dots are the seismic receivers. (a) show the fracture set # 1. These fracture plans are perpendicular to the *x*-axis at a spacing of 100 m, with depths from 3000 m to 3300 m and *y*-extent from -150 m to 150 m; (b) shows the fracture set #2, with depths from 3000 m to 3900 m and *y*-extent from -450 m to 450 m.

Numerical models and synthetic datasets

To assess the ability of single source acquisition in detecting fracture changes, we analyze two fracture models, horizontally extended fractures (Fracture set #1 in Figure 1a) and vertically extended fractures (Fracture set #2 in Figure 1b). A total of 961 3-component seismic nodes are distributed over a 3km x 3km rectangular area with a 100 m x 100 m spacing, while an explosive source is located at the center (Figure 1). The layered P-velocity, S-velocity, and density models are constructed based on a real well-log profile, with both fracture sets beginning at a depth of 3000

m. The synthetic data is generated using a 3D staggered-grid finite difference method for the elastic particle-velocity-stress wave equation (Fang et al. 2013, Fang et al. 2017). Fractures are modeled using the linear-slip boundary conditions with a constant compliance of $5x10^{-10}$ m/Pa (Schoenberg 1980, Schoenberg and Douma 1988). Figure 2 shows the recorded particle velocities (v_z and v_x) along two different profiles for the horizontally extended fractures (Figure 1a). In addition to hyperbolic reflection waves from layer discontinuities, fracture-related scattered waves are observed, with the horizontal components exhibiting relatively stronger amplitudes.

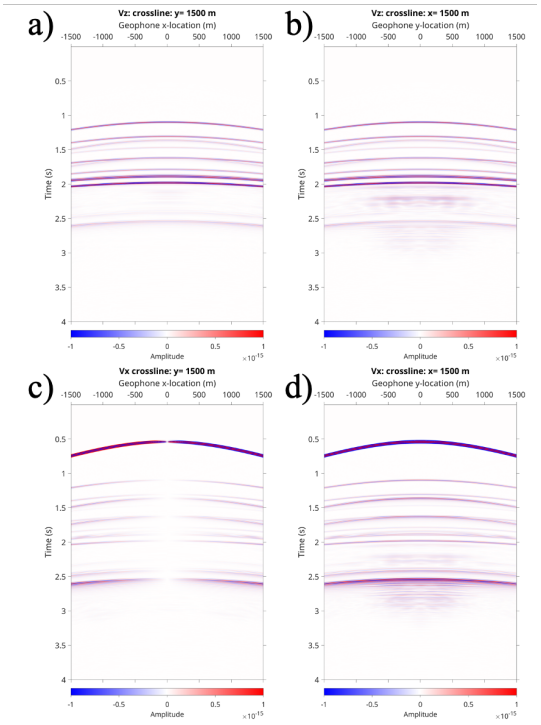

Figure 2. The synthetic common shot gathers. (a) and (b) are recorded z-components of particle-velocity (v_z) along y = 1500 m and x = 1500 m, respectively. (c) and (d) are recorded x-component of particle-velocity (v_x) along y = 1500 m, and x = 1500 m, respectively.

EDB results

We define the subsurface targets uniformly within a 3D volume, ranging from -400 m to 400 m in the x-direction, -600 m to 600 m in the y-direction, and 2500 m to 4000 m in depth (z), with a spacing of 50 m × 50 m × 50 m. We then apply the EDB method to each subsurface target and extract maximum amplitudes from each P-P and P-S_t DB image. Since the amplitude of the DB image is linearly proportional to the subsurface fracture compliance, it can be used to represent the inverted fracture relative "compliance".

To visualize the results, we present two cross-sectional profiles (one vertical and one horizontal) of the inverted fracture relative compliance in Figures 3 and 4, for two different fracture models, respectively. The results show strong agreement between the inverted fracture compliance maps and the actual spatial distribution of fractures in the model. From the comparison between Figures 3a and 4a, we can clearly observe changes in the horizontal extent of fractures. Similarly, Figures 3b and 4b effectively capture variations in fracture depth extent. It is worth pointing out that the EDB method cannot accurately invert targets located directly beneath the source, as the horizontal component of the vertically downgoing beam from the source become vanished. However, such cases are rare in field applications.

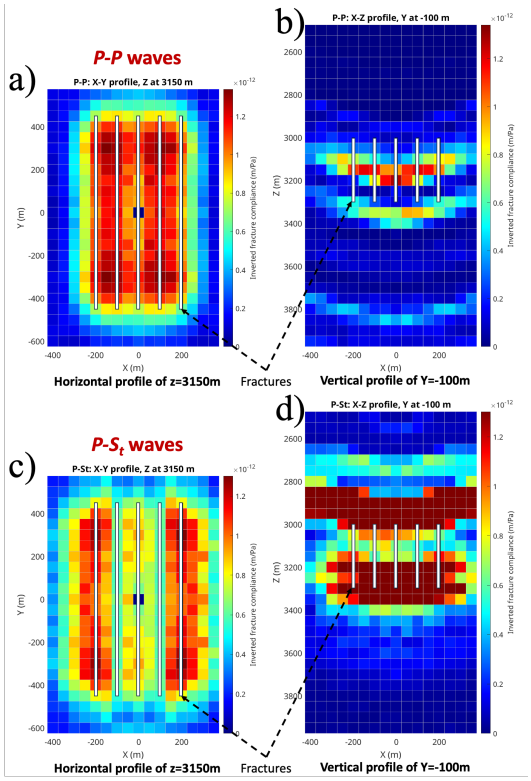

Figure 3. The inverted fracture compliance strength maps for the model in Figure 1a with horizontally extended fracture set #1. From P-P waves, (a) is the inverted compliance map for the horizontal (x-y) profile at the depth of 3150 m and (b) is the map for the vertical (x-z) profile at the y = -100 m. (c) and (d) are two profiles of inverted compliance maps from P-S_t waves. The white bars with black outlines indicate the true fracture planes.

Additionally, we present two examples of the EDB images at different subsurface targets in Figure 5. In Figures 5a and 5c, the absence of consistent and focused bright spots indicates a lack of preferentially aligned fractures at this target. Conversely,Figures 5b and 5d show well-focused and

10.1190/image2025-4301170.1

consistent bright spots with a normal direction of 0° and a spacing of approximately 100 m, which aligns with the fracture distribution in the model. These results confirm the effectiveness of the EDB method in accurately identifying fracture orientations and spatial extents.

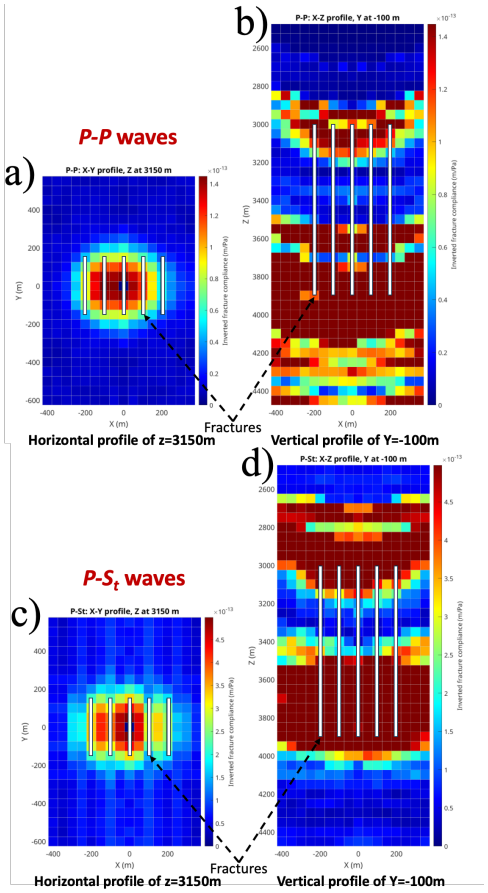

Figure 4. The inverted fracture compliance strength maps for the model in Figure 1b with vertically extended fracture set #2. (a) and (b) are the inverted compliance maps for the horizontal (x-y) profile at the depth of 3150 m and for the vertical (x-z) profile.

Discussion and Conclusions

The results from numerical simulations demonstrate the feasibility and reliability of the EDB method for detecting and characterizing subsurface fractures using a cost-effective 4D seismic acquisition with a single permanent source. By applying the EDB method to synthetic models containing distinct fracture sets, we successfully demonstrated its ability to resolve the spatial distribution of fractures and capture both horizontal and vertical fracture extents. Additionally, the observed variations in EDB images confirm the method's capability to differentiate between regions with and without preferentially aligned fractures. These results highlight the robustness of the EDB approach in providing high-resolution fracture characterization, even with a spatially sparse seismic acquisition setup featuring only one permanent source.

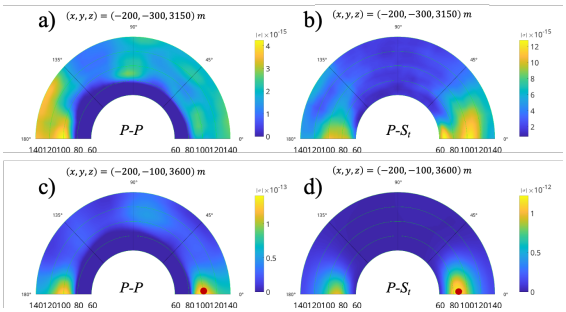

Figure 5. Inverted DB images for two selected targets in Model #2 with a beam width of 100 m at 45 Hz. (a) to (b) show the DB images of P-P, P-S_t waves for the target (x, y, z) at $(-200\ m, -300\ m, 3150\ m)$, respectively. In this target, there is no fracture in the model. The radius in the polar plot indicates the fracture spacing while the angle denotes the fracture plane's normal direction. (c) and (d) show the DB images of P-P and P-S_t waves for the target (x, y, z) at $(-200\ m, -100\ m, 3600\ m)$, respectively.

While the EDB method, combined with a cost-effective 4D seismic survey, presents a promising approach for monitoring subsurface fracture changes, certain limitations must be considered. The accuracy of the inverted fracture properties depends on the quality of seismic data and the accuracy of the velocity model. Additionally, the resolution of fracture characterization may be influenced by the complexity of subsurface structures and the level of noise present in real-world datasets. Further investigations should explore the integration of field data with more complex geological settings to assess the practical applicability of this approach.

In conclusion, the proposed solution integrating the EDB method and a cost-effective 4D seismic survey offers a reliable and cost-effective approach for monitoring dynamic changes in subsurface fractures. Its ability to accurately characterize fractures using a single repeated source and sparsely distributed seismic nodes makes it well-suited for applications such as reservoir monitoring, geothermal energy production, and carbon sequestration. Future work can focus on refining this method for real-world implementations and optimizing acquisition strategies to further enhance detection resolution, accuracy, and reliability.

Acknowledgments

The computing for this project was performed at the OU Supercomputing Center for Education & Research (OSCER) and Data Institute for Societal Challenges (DISC) at the University of Oklahoma (OU).

REFERENCES

Arts, R. J., X. Zhang, A. R. Verdel, D. Santonico, J. A. C. Meekes, R. P. Noorlandt, B. F. Paap, and V. P. Vandeweijer, 2013, Experiences with a permanently installed seismic monitoring array at the CO2 storage site at Ketzin (Germany). - A status overview: Energy Procedia, **37**, 4015–4023, doi: https://doi.org/10.1016/j.egypro.2013.06.301.

Barton, C. A., M. D. Zoback, and D. Moos, 1995, Fluid-flow along potentially active faults in crystalline rock. Geology, **23**, no. 8, 683–686, doi: https://doi.org/10.1130/0091-7613(1995)023<0683:FFAPAF>2.3.CO;2.

Berron, C., L. Michou, B. D. Cacqueray, F. Duret, J. Cotton, and E. Forgues, 2015, Permanent, continuous and unmanned 4D seismic monitoring: Peace River case study: 85th Annual International Meeting, SEG, Expanded Abstracts 2015, 5419–5423.

Caulk, R. A., E. Ghazanfari, J. N. Perdrial, and N. Perdrial. 2016, Experimental investigation of fracture aperture and permeability change within enhanced geothermal systems: Geothermics, **62**, 12–21, doi: https://doi.org/10.1016/j.geothermics.2016.02.003.

Crampin, S., 1985, Evaluation of anisotropy by shear-wave splitting: Geophysics, **50**, no. 1, 142–152, doi: https://doi.org/10.1190/1.1441824.

David, C., Y. Gueguen, and G. Pampoukis, 1990, Effective medium theory and network theory applied to the transport-properties of rock: Journal of Geophysical Research-Solid Earth and Planets, **95**, no. B5, 6993–7005, doi: https://doi.org/10.1029/JB095iB05p06993.

Fang, X., M. C. Fehler, Z. Zhu, Y. Zheng, and D. R. Burns, 2014a, Reservoir fracture characterization from seismic scattered waves: Geophysical Journal International, **196**, no. 1, 6993–7005, doi: https://doi.org/10.1029/JB095iB05p06993.

Fang, X., Y. Zheng, and M. Fehler, 2017, Fracture clustering effect on amplitude variation with offset and azimuth analyses: Geophysics, **82**, no. 1, N13–N25, doi: https://doi.org/10.1190/geo2016-0045.1.

Fang, X. D., M. Fehler, T. R. Chen, D. Burns, and Z. Y. Zhu, 2013, Sensitivity analysis of fracture scattering: Geophysics, **78**, no. 1, T1–T10, doi: https://doi.org/10.1190/geo2011-0521.1.

Fang, X. D., M. C. Fehler, Z. Y. Zhu, Y. C. Zheng, and D. R. Burns, 2014b, Reservoir fracture characterization from seismic scattered waves: Geophysical Journal International, **196**, no. 1, 481–492, doi: https://doi.org/10.1093/gji/ggt381.

Far, M. E., B. Hardage, and D. Wagner, 2014, Fracture parameter inversion for Marcellus Shale: Geophysics, **79**, no. 3, C55–C63, doi: https://doi.org/10.1190/geo2013-0236.1.

Harvey, S., J. Hopkins, H. Kuehl, S. O'Brien, and A. Mateeva, 2022, Quest CCS facility: Time-lapse seismic campaigns: International Journal of Greenhouse Gas Control, **117**, 103665.

Hu, H., A. AlAli, A. Almomin, and Y. Zheng, 2021, 3D seismic characterization of fractures using elastic P-to-S double-beams: Geophysics, 1–51, doi: https://doi.org/10.1190/geo2020-0830.1.

Hu, H., and Y. Zheng, 2017, 3D seismic characterization of fractures in a dipping reservoir layer by double beams: 87th Annual International Meeting, SEG, Expanded Abstracts, 3260–3266.

Hu, H., and Y. Zheng, 2018, 3D seismic characterization of fractures in a dipping layer using the double-beam method: Geophysics, **83**, no. 2, V123–V134, doi: https://doi.org/10.1190/geo2017-0435.1.

Hu, H., Y. Zheng, X. Fang, and M. C. Fehler, 2018, 3D seismic characterization of fractures with random spacing using the double-beam method: Geophysics, **83**, no. 5, M63–M74, doi: https://doi.org/10.1190/geo2017-0739.1.

Hu, H., Y. Zheng, L. Huang, and K. Gao, 2023, Imaging steeply dipping faults using angle-controlled decoupled elastic reverse-time migration of multicomponent seismic data: IEEE Transactions on Geoscience and Remote Sensing, **61**, 1–8.

Hubbert, M. K., and D. G. Willis, 1957, Mechanics of hydraulic fracturing: Transactions of the American Institute of Mining and Metallurgical Engineers, **210**, no. 6, 153–163.

Johnston, D., 1997, A tutorial on time-lapse seismic reservoir monitoring: Paper read at Offshore Technology Conference.

Klokov, A., and S. Fomel, 2012, Separation and imaging of seismic diffractions using migrated dip-angle gathers: Geophysics, **77**, no. 6, S131–S143, doi: https://doi.org/10.1190/geo2012-0017.1.

Landa, E., 2012, Seismic diffraction: where's the value?: 82nd Annual International Meeting, SEG, Expanded Abstracts, 1–4.

Landa, E., S. Fomel, and M. Reshef, 2008, Separation, imaging, and velocity analysis of seismic diffractions using migrated dip-angle gathers: 78th Annual International Meeting, SEG, Expanded Abstracts, 2176–2180.

Landa, E., A. Klokov, and R. Baina, 2011, Point and edge diffractions in three dimensions: Paper read at 73rd EAGE Conference and Exhibition incorporating SPE EUROPEC 2011.

Landa, E., G. Reshetova, and V. Tcheverda, 2013, Exploding reflectors revisited: 3D heterogeneous multiscale elastic media: 83rd Annual International Meeting, SEG, Expanded Abstracts, 3490-3494.

Long, M. D., 2013, Constraints on subduction geodynamics from seismic anisotropy: Reviews of Geophysics, **51**, no. 1, 76-112, doi: https://doi.org/10.1002/rog.20008.

Lynn, H. B., W. E. Beckham, K. M. Simon, C. R. Bates, M. Layman, and M. Jones, 1999, P-wave and S-wave azimuthal anisotropy at a naturally fractured gas reservoir, Bluebell-Altamont Field, Utah: Geophysics, **64**, no. 4, 1312–1328, doi: https://doi.org/10.1190/1.1444636.

Meunier, J., F. Huguet, and P. Meynier, 2000, Reservoir monitoring using permanent sources and vertical receiver antennae: 70th Annual International Meeting, SEG, Expanded Abstracts.

Montgomery, C. T., and M. B. Smith, 2010, Hydraulic fracturing: History of an enduring technology: Journal of Petroleum Technology, **62**, no. 12, 26–40, doi: https://doi.org/10.2118/1210-0026-JPT.

Nakatsukasa, M., I. Kurosawa, A. Kato, M. Takanashi, D. J. White, and K. Worth, 2016, The performance of an ACROSS permanent seismic source for time lapse seismic at the aquistore CO_2 storage site: Paper read at International Petroleum Technology Conference.

Nelson, R. 2001, Geologic analysis of naturally fractured reservoirs: Gulf Professional Publishing.

Oghenekohwo, F., H. Wason, E. Esser, and F. J. Herrmann, 2017, Low-cost time-lapse seismic with distributed compressive sensing—Part 1: Exploiting common information among the vintages: Geophysics, **82**, no. 3, P1–P13.

Orangi, A., N. R. Nagarajan, M. M. Honarpour, and J. Rosenzweig, 2011, Unconventional shale oil and gas-condensate reservoir production, impact of rock, fluid, and hydraulic fractures: Paper read at SPE Hydraulic Fracturing Technology Conference.

Perez, M. A., R. L. Gibson, and M. N. Toksoz, 1999, Detection of fracture orientation using azimuthal variation of P-wave AVO responses: Geophysics, **64**, no. 4, 1253–1265, doi: https://doi.org/10.1190/1.1444632.

Protasov, M. I., G. V. Reshetova, and V. A. Tcheverda, 2016, Fracture detection by Gaussian beam imaging of seismic data and image spectrum analysis: Geophysical Prospecting, **64**, no. 1, 68–82, doi: https://doi.org/10.1111/1365-2478.12259.

Rüger, A., and I. Tsvankin, 1997, Using AVO for fracture detection: Analytic basis and practical solutions: The Leading Edge, **16**, no. 10, 1429–1434, doi: https://doi.org/10.1190/1.1437466.

Schoenberg, M., 1980, Elastic wave behavior across linear slip interfaces: Journal of the Acoustical Society of America, **68**, no. 5, 1516–1521, doi: https://doi.org/10.1121/1.385077.

Schoenberg, M., and J. Douma, 1988, Elastic wave-propagation in media with parallel fractures and aligned cracks: Geophysical Prospecting, **36**, no. 6, 571–590, doi: https://doi.org/10.1111/j.1365-2478.1988.tb02181.x.

Schoepp, A., S. Labonte, and E. Landa, 2015, Multifocusing 3D diffraction imaging for detection of fractured zones in mudstone reservoirs: Case history: Interpretation, **3**, no. 1, Sf31–Sf42, doi: https://doi.org/10.1190/INT-2014-0064.1.

Shang, X., and L. Huang, 2012, Optimal designs of time-lapse seismic surveys for monitoring CO2 leakage through fault zones: International Journal of Greenhouse Gas Control, **10**, 419–433, doi: https://doi.org/10.1016/j.ijggc.2012.07.006.

Shukla, R., P. Ranjith, A. Haque, and X. Choi, 2010, A review of studies on CO2 sequestration and caprock integrity: Fuel, **89**, no. 10, 2651–2664, doi: https://doi.org/10.1016/j.fuel.2010.05.012.

Silvestrov, I., R. Baina, and E. Landa, 2016, Poststack diffraction imaging using reverse-time migration: Geophysical Prospecting, **64**, no. 1, 129–142, doi: https://doi.org/10.1111/1365-2478.12280.
Spackman, T., and D. C. Lawton, 2018, Processing and analysis of data recorded from a buried permanent seismic source: CREWES Annual Reports.
Spackman, T. W., D. C. Lawton, and M. Bertram, 2019, Seismic data acquired with a novel, permanently-installed borehole seismic source: 89th Annual International Meeting, SEG, Expanded Abstracts.
Stewart, R. R., J. E. Gaiser, R. J. Brown, and D. C. Lawton, 2002, Converted-wave seismic exploration: methods: Geophysics, **67**, no. 5, 1348–1363, doi: https://doi.org/10.1190/1.1512781.
Stewart, R. R., J. E. Gaiser, R. J. Brown, and D. C. Lawton, 2003, Converted-wave seismic exploration: Applications: Geophysics, **68**, no. 1, 40–57, doi: https://doi.org/10.1190/1.1543193.
Tatham, R. H., M. D. Matthews, K. K. Sekharan, C. J. Wade, and L. M. Liro, 1992, A physical model study of shear-wave splitting and fracture intensity: Geophysics, **57**, no. 4, 647–652, doi: https://doi.org/10.1190/1.1443278.
Thomsen, L., 1999, Converted-wave reflection seismology over inhomogeneous, anisotropic media: Geophysics, **64**, no. 3, 678–690, doi: https://doi.org/10.1190/1.1444577.
Vasconcelos, I., and V. Grechka, 2007, Seismic characterization of multiple fracture sets at Rulison Field, Colorado: Geophysics, **72**, no. 2, B19–B30, doi: https://doi.org/10.1190/1.2436779.
Verdon, J. P., and A. Wustefeld, 2013, Measurement of the normal/tangential fracture compliance ratio (ZN/ZT) during hydraulic fracture stimulation using S-wave splitting data: Geophysical Prospecting, **61**, 461–475, doi: https://doi.org/10.1111/j.1365-2478.2012.01132.x.
Vetri, L., E. Loinger, J. Gaiser, A. Grandi, and H. Lynn, 2003, 3D/4C Emilio: Azimuth processing and anisotropy analysis in a fractured carbonate reservoir: The Leading Edge, **22**, no. 7, 675–679, doi: https://doi.org/10.1190/1.1599695.
White, D. J., L. A. N. Roach, and B. Roberts, 2015, Time-lapse seismic performance of a sparse permanent array: Experience from the aquistore CO_2 storage site: Geophysics, **80**, no. 2, WA35–WA48, doi: https://doi.org/10.1190/geo2014-0239.1.
Willis, M. E., D. R. Burns, R. Rao, B. Minsley, M. N. Toksoz, and L. Vetri, 2006, Spatial orientation and distribution of reservoir fractures from scattered seismic energy: Geophysics, **71**, no. 5, O43–O51, doi: https://doi.org/10.1190/1.2235977.
Zheng, Y. C., X. D. Fang, and M. C. Fehler, 2013, Seismic characterization of reservoirs with variable fracture spacing by double focusing Gaussian beams: 83rd Annual International Meeting, SEG, Expanded Abstracts, 2432–2438.
Zheng, Y. C., X. D. Fang, M. C. Fehler, and D. R. Burns, 2013, Seismic characterization of fractured reservoirs by focusing Gaussian beams: Geophysics, **78**, no. 4, A23–A28: doi: https://doi.org/10.1190/geo2012-0512.1.